Title
Lung tumourigenesis in a conditional Cul4A transgenic mouse model

Journal
The Journal of Pathology, 233(2)

ISSN
0022-3417

Authors
Yang, Yi-Lin
Hung, Ming-Szu
Wang, Yang
et al.

Publication Date
2014-06-01

DOI
10.1002/path.4352

Peer reviewed

Published in final edited form as:
J Pathol. 2014 June ; 233(2): 113–123. doi:10.1002/path.4352.

Lung Tumorigenesis in a Conditional *Cul4A* Transgenic Mouse Model

Yi-Lin Yang[1,*], **Ming-Szu Hung**[1,2,3,4,*], **Yang Wang**[1,5,*], **Jian Ni**[1,6], **Jian-Hua Mao**[7], **David Hsieh**[1], **Alfred Au**[8], **Atul Kumar**[1], **David Quigley**[1], **Li Tai Fang**[1], **Che-Chung Yeh**[1], **Zhidong Xu**[1], **David M. Jablons**[1], and **Liang You**[1]

Liang You: liang.you@ucsfmedctr.org

[1]Department of Surgery, Helen Diller Family Comprehensive Cancer Center, University of California, San Francisco, CA 94143, USA

[2]Division of Pulmonary and Critical Care Medicine, Chang Gung Memorial Hospital, Chiayi, Taiwan

[3]Department of Medicine, College of Medicine, Chang Gung University, Taoyuan, Taiwan

[4]Department of Respiratory Care, Chang Gung University of Science and Technology, Chiayi Campus, Chiayi, Taiwan

[5]Department of Thoracic Surgery, Beijing Chao-Yang Hospital, Capital University of Medical Science, Beijing, 100020, PRC

[6]Department of Oncology, Shanghai Pulmonary Hospital, Tongji University School of Medicine, Shanghai, 200050, PRC

[7]Life Sciences Division, Lawrence Berkeley National Laboratory, University of California, Berkeley, CA USA

[8]Division of Diagnostic Pathology, Helen Diller Family Comprehensive Cancer Center, University of California, San Francisco, CA 94143, USA

Abstract

Cullin4A (Cul4A) is a scaffold protein that assembles cullin-RING ubiquitin ligase (E3) complexes and regulates many cellular events, including cell survival, development, growth, and cell cycle control. Our previous study suggested that *Cul4A* is oncogenic *in vitro*, but its oncogenic role *in vivo* has not been studied. Here, we used a *Cul4A* transgenic mouse model to study the potential oncogenic role of *Cul4A* in lung tumor development. After *Cul4A* overexpression was induced in the lungs for 32 weeks, atypical epithelial cells were observed. After 40 weeks, lung tumors were visible and were characterized as Grade I or II adenocarcinomas.

Corresponding author: Liang You (Liang.You@ucsfmedctr.org) Department of Surgery, Helen Diller Family Comprehensive Cancer Center, University of California, San Francisco, 2340 Sutter Street, N-221, San Francisco, CA 94115, Telephone: 415-476-6906 Fax: 415-514-1074.
*The authors contributed equally to this work.

Conflict of Interest Statement: The authors have no declared conflicts of interest.

Author Contributions

YY, MH, YW, DH and ZX performed the research; YY, MH, YW, NJ, DH, AA, AK, DQ, LF, CY, CP, ZX, DMJ, and LY analyzed data; YY, MH, YW and LY designed the research and wrote the paper.

Immunohistochemistry (IHC) revealed decreased levels of *Cul4A* associated proteins $p21^{CIP1}$ and tumor suppressor $p19^{ARF}$ in the lung tumors, suggesting Cul4A regulated their expression in these tumors. Increased levels of $p27^{KIP1}$ and $p16^{INK4a}$ were also detected in these tumors. Moreover, protein level of DNA replication licensing factor CDT1 was decreased. Genomic instability in the lung tumors was further analyzed by the results from pericentrin protein expression and array Comparative Genomic Hybridization analysis. Furthermore, knocking down *Cul4A* expression in lung cancer H2170 cells increased their sensitivity to the chemotherapy drug cisplatin *in vitro*, suggesting that *Cul4A* overexpression is associated with cisplatin resistance in the cancer cells. Our findings indicate that *Cul4A* is oncogenic *in vivo*, and this *Cul4A* mouse model is a tool in understanding the mechanisms of *Cul4A* in human cancers and for testing experimental therapies targeting *Cul4A*.

Keywords

non-small cell lung cancer; *Cul4A*; Ad-Cre; transgenic mouse models; cell cycle

Introduction

The Cullin4A gene (*Cul4A*) is overexpressed or amplified in a variety of human cancers [1–4]. Association of *Cul4A* amplification with aggressive tumor growth and poor prognosis has been suggested [5, 6]. *Cul4A* depletion reportedly increased the protection of mouse skin from ultraviolet-induced carcinogenesis [7]. We previously demonstrated the amplification of *Cul4A* copy number and the increased expression of Cul4A protein in malignant pleural mesothelioma cells, suggesting that *Cul4A* is an oncogene in thoracic cancer [8]. However, the oncogenic role of *Cul4A in vivo* has not been studied.

Recently, amplification of *Cul4A* and other genes was detected on chromosome 13q34 using fluorescence *in situ* hybridization (FISH) and the frequency of occurrence was 3% in human non-small cell lung cancer (NSCLC) [9]. Amplification of *Cul4A* in lung cancer was further supported by our analysis of the Cancer Genome Atlas (TCGA) data using the Oncomine cancer microarray database (www.oncomine.org)[10]. *Cul4A* copy number increased by 1.4 fold (≥ 3 copies) in 3% of lung adenocarcinomas (n=138) (Supplementary Fig. 1) and in 3% of lung squamous cell carcinomas (n=204) (Supplementary Fig. 2) when compared to normal lung tissues. Our analysis of TCGA data using the cBioPortal for Cancer Genomics database (http://www.cbioportal.org)[11, 12] further revealed the up-regulation of *Cul4A* in 8.3% of lung squamous cell carcinoma (n=179) and in 6% of lung adenocarcinoma (n=230) (data not shown). We also found a correlation between *Cul4A* mRNA expression levels and *Cul4A* copy number in lung adenocarcinoma cases (Supplementary Fig. 3). Collectively, these results suggest that increased expression of *Cul4A* is associated with the occurrence of lung cancer in humans, but its oncogenic role *in vivo* remains to be investigated.

To investigate the biology of the ≥ 3% of NSCLC that showed *Cul4A* overexpression, we developed a Lox–Stop–Lox *Cul4A* conditional mouse strain (*Lox-Cul4A*) [13], in which *Cul4A* overexpression is activated by the introduction of an engineered adenovirus carrying the Cre recombinase (Ad-Cre) [14]. After *Cul4A* overexpression was induced, we observed

lesions after 24 weeks and visible lung tumors after 40 weeks. Mouse lungs and lung tumors were collected at several time points after *Cul4A* overexpression and analyzed for the expression of Cul4A protein and its associated proteins. Here, we show that *Cul4A* is oncogenic *in vivo* and that overexpression of *Cul4A* leads to tumorigenesis in the mouse lung.

Materials and Methods

Induction of Cul4A-overexpression in transgenic mice

All *in vivo* experiments strictly followed the UCSF institutional guidelines (Institutional Animal Care and Use Committee approval number: AN085516-03C). The *Cul4A* transgenic mice were generated as previously described [13] and were maintained as heterozygotes on an FVB/N background. The engineered adenovirus (Ad) carrying either Cre-recombinase (Ad5CMVCre) or GFP (Ad5CMVeGFP) was purchased from the Gene Transfer Vector Core of the University of Iowa. The adenoviruses were introduced into the 6–10 week-old mice through inhalation to induce *Cul4A* overexpression in lung as previously described [15]. Age-matched littermate mice infected with Ad-GFP were used as controls. Transgenic mice were anesthetized with 2.5% Avertin via intraperitoneal injection, after which half of the mice inhaled approximately 10^6 or 10^7 particles of Ad-Cre or Ad-GFP directly into the lungs.

Histological and immunohistochemical analysis (IHC) of lung and tumor samples

Lungs from the transgenic mice were collected at 8, 16, 24, 32, 40, 48, 56, and 64 weeks after infection with the adenovirus. Lung tumors were collected at 40, 48, 56, and 64 weeks after infection with the adenovirus. Histological sections of the mouse lungs and lung tumors were stained with hematoxylin and eosin for general morphology analysis. For IHC analysis, endogenous peroxidase was quenched for 15 min at room temperature with 3% H_2O_2 in methanol in each lung section. Sections were blocked with 4% normal goat serum in PBS with 0.2% Triton for two hours at room temperature before incubation overnight at 4°C with the properly diluted antibodies: anti-Cul4A (ab34897,Abcam) at 1:400; anti-c-Myc (sc-789, Santa Cruz) at 1:20; anti-PCNA (sc-7907, Santa Cruz) at 1:100; anti- $p21^{CIP1}$ (sc-471, Santa Cruz) at 1:100; anti- $p27^{KIP1}$ (sc-528, Santa Cruz) at 1:100; anti- $p14/19^{ARF}$ (251543,Abbiotec) at 1:100; anti-p16 (sc-1207, Santa Cruz) at 1:200; anti-CDT1 (ab70829,Abcam) at 1:250; anti-pericentrin (ab4448,Abcam) at 1:2000.

Three independent researchers blindly scored positivity, and the data represent the samples that were scored positive by all three individuals. The following scoring system was used: −, no stain; +, weak staining (10% or above stained cellularity considered as positive); ++, moderate staining (30% or above stained cellularity considered as positive); +++, strong staining (50% or above stained cellularity considered as positive). All scoring was done under magnification (20×) with a Zeiss Axioscop 2 microscope (Carl Zeiss Inc, Germany) and photomicrographs were obtained with a Carl Zeiss AxioCam MrC5 camera.

Cell viability assay

The CellTiter-Glo® luminescent cell viability assay (Promega, Madison, WI) was used to evaluate cisplatin cytotoxicity. H2170 cells were transfected with *Cul4A* siRNA or control siRNA at 100nM, 50nM, or 1nM using Lipofectamine RNAiMAX (Invitrogen, Carlsbad, CA, USA) according to the manufacturer's protocol. H838 and H460 cells were transfected with Cul4A siRNA or control siRNA at 50nM. Transfected cells were seeded at 5000 cells/well in 96-well plates and cultured at 37°C supplied with 5% CO_2 without antibiotics for 24 hours. Cells were treated with cisplatin (10 fold serial dilution) for 72 hours. Then, 50 μl of the CellTiter-Glo reagent was added into each well. After incubation for 10 minutes, the luminescence signals were read by a GloMax® 96 microplate luminometer (Promega, Madison, WI) and a dose–response curve was plotted. The assay was done in triplicate and data are shown as mean values ± standard deviation (SD). The half maximal inhibitory concentration (IC_{50}) values were determined using GraphPad Prism® log (inhibitor) vs. response (variable slope) software (version 6.01, La Jolla, CA). Paired Student's t-tests were used to compare cell viability for different treatments against the samples with cisplatin only. Significance was defined as $p < 0.05$ with two-sided analysis.

Results

Lesions and tumors in the transgenic mouse lung

To determine whether overexpressing *Cul4A* resulted in tumor development in mouse lungs, we generated heterozygous transgenic mice overexpressing Cre-inducible *Cul4A (Lox-Cul4A)*[13], collected mouse lungs after *Cul4A* overexpression was induced (Fig. 1A), and analyzed tissue sections from mouse lungs by using IHC. We found that the morphology of Ad-GFP induced mouse lung appeared to be normal at all time points (Fig. 1B). In contrast, mice injected with Ad-Cre showed hyperplasia after 8 to 16 weeks of *Cul4A* overexpression, as was noted previously [13]. Local edema was evident at 24 weeks and notably worse at 40 weeks (Fig. 1C). Multiple aggregations of lymphocytes were observed under the respiratory epithelial lining (Fig. 1D). The number and size of the lymphocyte aggregations increased after 24 weeks of *Cul4A* overexpression (Fig. 1E). We observed small groups of atypical cells at 32 weeks (Fig. 1F) and larger groups of these cells at 40 weeks (Fig. 1G), whereas the morphology of the surrounding bronchial epithelium appeared normal. The atypical epithelial cells showed enlarged nuclei and cell size, suggesting that these cells may develop into tumor cells at later time points.

We observed tumors on the surface of 8/25 (32%) mouse lungs after 40 weeks of *Cul4A* overexpression. One of these eight lungs had two tumors. These nine tumors ranged in size from 2.25 to 25 mm^2 (Fig. 2A, T1–T9), and all of the tumor cells showed numerous mitoses and enlarged nuclei and progressed to glandular structures. Three of the nine tumors were characterized as Grade I adenocarcinoma with well-differentiated cell structure (Fig. 2B, D), generally considered the least aggressive tumor cells. Five of the nine tumors were intermediate grade with moderately differentiated tumor cells (Fig. 2C, E). The Grade II tumors also showed breakthrough of the tumor barrier (Fig. 3A) and lymphovascular infiltration (Fig. 3B), suggesting invasive behavior and spread to the lymphatics. In addition, in the tissue surrounding the major tumor, we observed satellite adenocarcinomas with

invasion to adjacent stroma after 64 weeks of *Cul4A* overexpression (Fig. 3C). Multiple lymphoid aggregates surrounded the developed adenocarcinoma (Fig. 3D), suggesting that their appearance is associated with tumor development. These results show that adenocarcinoma growth can be induced in this mouse model and that the tumors have developed invasive behavior and can multiply in the mouse lung. Moreover, increased expression of Cul4A and the *c-Myc* tag, which was constructed after the *Cul4A* transgene, was detected in the mouse lung tumors (Supplementary Fig.4A–B). Quantitative analysis of the IHC data for Cul4A, $p27^{KIP1}$, CDT1 and pericentrin showed similar trend of changes in IHC staining intensity between lung tumors and control lungs (Supplementary Fig. 4C). Copy number of the *Cul4A* transgene in the transgenic mouse tissues was analyzed by using qPCR (Supplementary Fig. 5A). Similar *Cul4A* copy number (3–4 copies) was detected in the mouse lungs and in the MEFs whereas the lung tumors showed similar or slightly more *Cul4A* copy number in the cells.

Decreased expression of $p21^{CIP1}$ and increased expression of PCNA in the lung tumors overexpressing *Cul4A*

To further study the possible mechanism of Cul4A, a component of Cul4A-based E3 ubiquitin ligase complexes, on the development of lung adenocarcinoma, we analyzed the expression of several proteins, which are known to associate with Cul4A, in the lungs and tumor samples from mice that overexpressed human *Cul4A* transgene. The cyclin-dependent kinase (CDK) inhibitor $p21^{CIP1}$ has been shown to associate with Cul4A-based E3 ubiquitin ligase complex [16, 17]. We previously demonstrated that Cul4A overexpression resulted in downregulation of $p21^{CIP1}$ protein in mesothelioma cells [8], suggesting that Cul4A overexpression mediated the degradation of $p21^{CIP1}$ *in vitro*. In this *Lox-Cul4A* mouse model, $p21^{CIP1}$ protein expression in control lungs was strong at every time point (Fig. 4A, inset) but weak in the six tumors examined (Fig. 4A, main figure). Both chromosomal and transcriptional levels of $p21^{CIP1}$ measured in the lung tumors and the mouse lungs using qRT-PCR showed similar results (Supplementary Fig. 5B), suggesting the decrease in $p21^{CIP1}$ expression occurred in the post-translational level. These IHC results suggest that *Cul4A* overexpression decreased $p21^{CIP1}$ expression in the lung tumors, an event which may be associated with lung tumor development in this mouse model. We next used the MEFs from transgenic mice to evaluate the observation of $p21^{CIP1}$ degradation driven by *Cul4A* overexpression. Primary mouse MEFs generated from the transgenic mouse model were infected with Ad-Cre to induce *Cul4A* overexpression. Afterward, the cells were co-transfected with HA-tagged $p21^{CIP1}$ and either *Cul4A* siRNA or control siRNA. Our results indicate that the expression of $p21^{CIP1}$ was increased in the cells when *Cul4A* expression was knocked down (Fig. 4B). To test the possible mechanism that decreased $p21^{CIP1}$ expression in the lung tumors, we next examined the expression of PCNA, a key co-factor that mediates Cul4A-dependent proteolysis of $p21^{CIP1}$ [16, 18]. IHC analysis revealed that PCNA expression was strong in the four lung tumors analyzed (Fig. 4C, main figure) but weak in the control lungs (Fig. 4C, inset), suggesting that elevated PCNA expression contributed to Cul4A-mediated $p21^{CIP1}$ downregulation in lung tumorigenesis.

Expression of tumor suppressors from the INK4a/ARF locus in the lung tumors

Considering that the INK4a/ARF locus encodes tumor suppressor genes that play a pivotal role in controlling the RB/p53 network, we next analyzed the expression of $p19^{ARF}$ ($p14^{ARF}$ in human) and $p16^{INK4a}$ in the lung tumors overexpressing *Cul4A*. IHC analysis revealed that $p19^{ARF}$ expression was weak in the seven analyzed tumors (Fig. 4D, main figure) when compared to that in the control lungs (Fig. 4D, inset). In contrast, $p16^{INK4a}$ expression was strong in the lung tumors (Fig. 4E, main figure) but weak in the control lungs (Fig. 4E, inset).

Increased expression of $p27^{KIP1}$ in the lung tumors

Protein $p27^{KIP1}$ is a key regulator of cell-cycle progression, and can regulate cell-cycle arrest by inhibiting CDK activity [19]. Protein $p27^{KIP1}$ may be a prognostic factor in human cancers [20–22] and its depletion in mice results in tumor growth [23]. Moreover, Cul4A-based E3 ubiquitin ligase was shown to mediate the expression of $p27^{KIP1}$ [24]. In our mouse model, $p27^{KIP1}$ expression was strong in the lung tumors overexpressing *Cul4A* (Fig. 4F, main figure) but moderate in the control lungs (Fig. 4F, inset). These results suggest that *Cul4A* overexpression elevated $p27^{KIP1}$ expression in lung tumorigenesis.

Genomic instability in the lung tumors that overexpressed *Cul4A*

As a key factor in regulating genetic stability, DNA replication licensing factor CDT1 can also associate with Cul4A-based E3 ubiquitin ligase complexes [25–27]. To determine whether overexpression of *Cul4A* resulted in loss of CDT1 expression, we compared CDT1 expression in lung tumors and control lungs by using IHC analysis. Expression of CDT1 was negative in the six lung tumors (Fig. 5A, main figure) but moderate in the control lungs (Fig. 5A, inset). Both chromosomal and transcriptional levels of *CDT1* measured in the lung tumors and the mouse lungs by using qRT-PCR showed similar results (Supplementary Fig. 5C), suggesting the decrease of CDT1 expression occurred in the post-translational level. We next measured the expression of CDT1 in primary MEFs using western blotting and our results showed that knocking down *Cul4A* expression using siRNA decreased Cul4A expression but increased CDT1 expression in the cells (Fig. 5B). Together, the results suggested that CDT1 expression was decreased in the lung tumors overexpressing *Cul4A*. To test whether genomic instability occurred in the lung tumors, the expression of pericentrin, an indicator of genomic instability [28], was analyzed using IHC. Our data showed that pericentrin expression was strong in the lung tumors (Fig. 5C, main figure) but weak in control lungs (Fig. 5C, inset), suggesting genomic instability occurred in the lung tumors overexpressing *Cul4A*.

The genomic instability in the tumors that overexpress *Cul4A* was further evaluated using array Comparative Genomic Hybridization (aCGH) to visualize DNA copy number alterations across the lung tumor genomes. The most frequent amplification was on distal chromosome 8 and the most frequent deletion was on proximal chromosome 18 (Fig. 5D). *Kras* transgenic mouse model of lung cancer was developed and genomic instability in the lung tumors was analyzed using aCGH [29]. Increase in DNA copy number was detected on multiple chromosomes in the aCGH results collected from *Kras* overexpressed lung tumors. Similar to our observation of the aCGH data from *Cul4A* overexpressed lung tumors,

increase in DNA copy number was also detected on the chromosome 8 of *Kras* overexpressed tumors. Genomic instability was also shown in human NSCLC cell lines H2170 (4 copies) and H226 (3 copies)(Fig. 6A) analyzed by using aCGH [30]. High level of amplification at 8q24 was identified in both H2170 and H226 cells. Additional amplification was also identified in H2170 cells at 14q13. These results suggest that recurring DNA copy alterations occurred during tumorigenesis in this *Cul4A* mouse model. However, further study with a larger sample size of tumors is needed to confirm this hypothesis.

A synergistic effect in inhibiting NSCLC by *Cul4A* knock down and cisplatin treatment

We next examined whether *Cul4A* overexpression is associated with drug resistance to the chemotherapy drug cisplatin in NSCLC. To test this hypothesis, we knocked down *Cul4A* expression in NSCLC using RNA interference and then measured the sensitivity of these NSCLC cells to cisplatin treatment. Among the six lung cancer cell lines expressing moderate to high levels of Cul4A compared to the weak Cul4A expression in the normal lung as shown by IHC analysis, the H2170 cell line had the highest copy number of *Cul4A* when analyzed using FISH (Fig. 6A). We next compared the inhibition effects of cisplatin on H2170 with or without *Cul4A* siRNA. The inhibition efficiency of RNA interference on *Cul4A* mRNA transcription was over 94% in four selected cancer cell lines (Supplementary Fig. 5A). Viability of H2170 cells was measured after 72 hours of cisplatin treatment (Fig. 6B, C). From the dose response curve, IC_{50} values were calculated in H2170 cells treated with cisplatin and either 100nM *Cul4A* siRNA (0.91 ± 5.8 μM), 100nM control siRNA (2.34 ± 5.5 μM), 1nM *Cul4A* siRNA (2.48 ± 5.1 μM), or 1nM control siRNA (2.31 ± 6.5 μM) (Fig. 6D). IC_{50} values in H2170 cells treated with cisplatin only averaged 3.35 ± 5.3 μM. We further compared the effect of the combination treatment in NSCLC cell lines H460, H838, and H2170 using the combination treatment of 50 nM *Cul4A* siRNA and cisplatin (Supplementary Fig. 6B–D), and all the NSCLC cell lines showed increased in their sensitivity to cisplatin when the *Cul4A* expression was knocked down. From the dose response curve, the IC_{50} values in H2170 cells (higher *Cul4A* copy number) decreased ~20% when *Cul4A* was knocked down, and the IC_{50} values in H460 or H838 cell lines (lower *Cul4A* copy number) was decreased ≤ 3% when *Cul4A* was knocked down (Supplementary Fig. 6E). Together, these results suggest that the combination treatment of *Cul4A* knock down and cisplatin showed a synergistic effect in inhibiting NSCLC cells.

Discussion

Our study demonstrates that *Cul4A* is oncogenic *in vivo* and that the development of lung tumors can be induced by *Cul4A* overexpression. After *Cul4A* was overexpressed in lung tumors, the protein levels of $p21^{CIP1}$, $p19^{ARF}$ and CDT1 decreased, whereas those of $p27^{KIP1}$, $p16^{INK4a}$, PCNA, and pericentrin increased. Our results suggest that these cellular events contribute to the initiation and development of the lung tumors in the mouse model of *Cul4A* overexpression, and that the expression of DNA replication licensing factor CDT1 may contribute to genomic instability and tumor development. Our study also showed that in addition to the oncogenic role of *Cul4A* expression *in vivo*, knocking down *Cul4A* expression in lung cancer H2170 cells increased their sensitivity to the chemotherapy drug cisplatin.

In IHC analysis of six human NSCLC cell lines, H2170 cells with four *Cul4A* copy numbers analyzed using FISH showed strong Cul4A staining score (+++)(Fig 6A). H226 and H345 cells with three *Cul4A* copy numbers showed strong to moderate IHC staining score (+++ and ++, respectively). H838, A549 and H460 cells with two *Cul4A* copy numbers showed moderate IHC staining score (++). In contract, normal lung tissue showed weak Cul4A staining score (+/−) (data not shown). We believe that our mouse model represents, at least in part, a fraction of human NSCLC with amplified Cul4A copy number.

Our IHC analysis indicated that the level of $p27^{KIP1}$ expression was increased in lung tumors overexpressing *Cul4A*, suggesting that $p27^{KIP1}$ is probably not proteolyzed by Cul4A-based E3 ubiquitin ligase in the lung tumors. This finding is supported by previous studies suggesting that $p27^{KIP1}$ is not a target degraded by the Cul4A-based E3 ubiquitin ligase [31, 32]. For instance, depletion of the Cul4A-RING ubiquitin ligase (E3) complexes did not immediately increase $p27^{KIP1}$ expression in the cells [31, 32]. In addition, $p27^{KIP1}$ expression was elevated in response to UV-irradiation, regardless the presence of functional Cul4A-based E3 ubiquitin ligase complex in the cells [32]. Together, these findings and ours all suggest that $p27^{KIP1}$ is not a target degraded by Cul4A-based E3 ubiquitin ligase. Because $p27^{KIP1}$ functions as a tumor suppressor and was strongly expressed in our *Cul4A* mouse model, knocking down the expression of $p27^{KIP1}$ in our mouse model could provide further insights into the biology of human cancers that overexpress *Cul4A*.

It has been shown that Cul4A-based E3 ubiquitin ligase complex is required for $p16^{INK4a}$ activation in human lung cells [33]. In clinical studies, inactivation of $p16^{INK4a}$ was reported in 40% to 70% of human NSCLC cases [34, 35]. Interestingly, $p16^{INK4a}$ expression was not decreased in the lung tumors of our *Cul4A* mouse model, suggesting that downregulation of $p16^{INK4a}$ expression in this model could provide further insights into the biology of *Cul4A*-mediated tumorigenesis. Therefore, by crossing this mouse model with a $p16^{INK4a}$ knockout strain, we generated a new mouse model that has $p16^{INK4a}$ depletion and oncogenic *Cul4A* overexpression. This new model provides an excellent opportunity to improve our understanding of the biology of cancers in which *Cul4A* is overexpressed, including NSCLC, mesothelioma, breast cancer, and skin carcinomas.

The results of our IHC analysis showed decreased expression of $p19^{ARF}$ in the lung tumors overexpressing *Cul4A*. This finding suggests that degradation of $p19^{ARF}$ protein occurred after *Cul4A* overexpression and that the loss of $p19^{ARF}$ may contribute to tumor development in this mouse model.

$p21^{CIP1}$ deficient mice have been shown to develop different tumors in the mouse organs, including lung carcinomas [36]. Because Cul4A can target multiple different proteins for degradation (Fig. 7), the phenotype of *Cul4A* transgenic mice is expected to be more tumorigenic than that in the $p21^{CIP1}$ deficient mice.

The role *Cul4A* plays in the initiation and development of lung tumors in our mouse model has implications for understanding cancer biology and introduces new avenues for therapeutic development targeting *Cul4A*. These possibilities are supported by recent findings that MLN4924, a small molecule that blocks the activation of Cullin-based E3

ubiquitin ligase, suppresses tumor cell growth [37]. The effect of MLN4924 in controlling the growth of lung tumors can be further investigated in our mouse model. To date, cisplatin, a platinum-based therapy, is one of the most commonly used chemotherapeutic agents in the treatment of NSCLC, but about 20% of patients experience a partial response to cisplatin [38, 39]. Our study found that the IC_{50} of NSCLC cell line H2170 decreased more than two-fold when *Cul4A* transcription was knocked down before the cisplatin treatment, suggesting that *Cul4A* overexpression is associated with cisplatin resistance in the cancer cells. This possibility is supported by the fact that a combination therapy consisting of MLN4924 and cisplatin significantly reduces tumor burden in mice, a finding that also suggests a mechanism to induce cancer cell apoptosis by trigging ROS production to induce DNA damage in cancer cells [40]. Whether this mechanism is involved in the decreased cell viability in the H2170 cells treated with both *Cul4A* siRNA and cisplatin remains to be examined.

In summary, the *Cul4A* mouse model described here has many advantages over existing mouse models for cancer research. The ability to target specific organs through localized Ad-Cre infection can be useful to generate mouse models for studying the development of organ-specific tumors. Using this mouse model, we demonstrated for the first time that *Cul4A* is oncogenic *in vivo* and that the development of lung tumors can be induced by *Cul4A* overexpression. From these findings, we conclude that overexpression of *Cul4A* plays a role in tumor development in this mouse model (Fig. 7). A better understanding of the mechanisms of *Cul4A*-mediated lung tumorigenesis in this mouse model could provide new insights into the biology of human cancers that overexpress *Cul4A* and could contribute to future experimental therapies.

Supplementary Material

Refer to Web version on PubMed Central for supplementary material.

Acknowledgments

The present work was supported by NIH grant R01 CA140654-01A1 (LY). We are grateful for support from the Kazan, McClain, Abrams, Fernandez, Lyons, Greenwood, Harley & Oberman Foundation, Inc; the Estate of Robert Griffiths; the Jeffrey and Karen Peterson Family Foundation; Paul and Michelle Zygielbaum; the Estate of Norman Mancini; and the Barbara Isackson Lung Cancer Research Fund. We specially thank Osamu Tetsu, Ph.D. from UCSF Cancer Center for kindly provide the HA-p21CIP1-pcDNA3 plasmid as a gift. We thank Loretta Chan in the UCSF Cancer Center Tissue Core for her help. We also thank Pamela Derish in the UCSF Department of Surgery for editorial assistance with the manuscript.

Abbreviations

Cul4A	Cullin4A
NSCLC	non-small cell lung cancer
FISH	fluorescence *in situ* hybridization
TCGA	The Cancer Genome Atlas
Ad-Cre	engineered adenovirus carrying the Cre recombinase

IHC	immunohistochemistry
aCGH	array Comparative Genomic Hybridization

References

1. Chen LC, Manjeshwar S, Lu Y, et al. The human homologue for the Caenorhabditis elegans cul-4 gene is amplified and overexpressed in primary breast cancers. Cancer Res. 1998; 58:3677–3683. [PubMed: 9721878]
2. Shinomiya T, Mori T, Ariyama Y, et al. Comparative genomic hybridization of squamous cell carcinoma of the esophagus: the possible involvement of the DPI gene in the 13q34 amplicon. Genes Chromosomes Cancer. 1999; 24:337–344. [PubMed: 10092132]
3. Yasui K, Arii S, Zhao C, et al. TFDP1, CUL4A, and CDC16 identified as targets for amplification at 13q34 in hepatocellular carcinomas. Hepatology. 2002; 35:1476–1484. [PubMed: 12029633]
4. Abba MC, Fabris VT, Hu Y, et al. Identification of novel amplification gene targets in mouse and human breast cancer at a syntenic cluster mapping to mouse ch8A1 and human ch13q34. Cancer Res. 2007; 67:4104–4112. [PubMed: 17483321]
5. Melchor L, Saucedo-Cuevas LP, Munoz-Repeto I, et al. Comprehensive characterization of the DNA amplification at 13q34 in human breast cancer reveals TFDP1 and CUL4A as likely candidate target genes. Breast Cancer Res. 2009; 11:R86. [PubMed: 19995430]
6. Ren S, Xu C, Cui Z, et al. Oncogenic CUL4A determines the response to thalidomide treatment in prostate cancer. J Mol Med (Berl). 2012; 90:1121–1132. [PubMed: 22422151]
7. Liu L, Lee S, Zhang J, et al. CUL4A abrogation augments DNA damage response and protection against skin carcinogenesis. Mol Cell. 2009; 34:451–460. [PubMed: 19481525]
8. Hung MS, Mao JH, Xu Z, et al. Cul4A is an oncogene in malignant pleural mesothelioma. J Cell Mol Med. 2011; 15:350–358. [PubMed: 19929949]
9. Castillo SD, Angulo B, Suarez-Gauthier A, et al. Gene amplification of the transcription factor DP1 and CTNND1 in human lung cancer. J Pathol. 2010; 222:89–98. [PubMed: 20556744]
10. Rhodes DR, Kalyana-Sundaram S, Mahavisno V, et al. Oncomine 3.0: genes, pathways, and networks in a collection of 18,000 cancer gene expression profiles. Neoplasia. 2007; 9:166–180. [PubMed: 17356713]
11. Cerami E, Gao J, Dogrusoz U, et al. The cBio cancer genomics portal: an open platform for exploring multidimensional cancer genomics data. Cancer Discov. 2012; 2:401–404. [PubMed: 22588877]
12. Gao J, Aksoy BA, Dogrusoz U, et al. Integrative analysis of complex cancer genomics and clinical profiles using the cBioPortal. Sci Signal. 2013; 6:pl1. [PubMed: 23550210]
13. Li T, Hung MS, Wang Y, et al. Transgenic mice for cre-inducible overexpression of the Cul4A gene. Genesis. 2011; 49:134–141. [PubMed: 21381181]
14. Jackson EL, Willis N, Mercer K, et al. Analysis of lung tumor initiation and progression using conditional expression of oncogenic K-ras. Genes Dev. 2001; 15:3243–3248. [PubMed: 11751630]
15. DuPage M, Dooley AL, Jacks T. Conditional mouse lung cancer models using adenoviral or lentiviral delivery of Cre recombinase. Nat Protoc. 2009; 4:1064–1072. [PubMed: 19561589]
16. Abbas T, Sivaprasad U, Terai K, et al. PCNA-dependent regulation of p21 ubiquitylation and degradation via the CRL4Cdt2 ubiquitin ligase complex. Genes Dev. 2008; 22:2496–2506. [PubMed: 18794347]
17. Kim Y, Starostina NG, Kipreos ET. The CRL4Cdt2 ubiquitin ligase targets the degradation of p21Cip1 to control replication licensing. Genes Dev. 2008; 22:2507–2519. [PubMed: 18794348]
18. Nishitani H, Shiomi Y, Iida H, et al. CDK inhibitor p21 is degraded by a proliferating cell nuclear antigen-coupled Cul4-DDB1Cdt2 pathway during S phase and after UV irradiation. J Biol Chem. 2008; 283:29045–29052. [PubMed: 18703516]

19. Toyoshima H, Hunter T. p27, a novel inhibitor of G1 cyclin-Cdk protein kinase activity, is related to p21. Cell. 1994; 78:67–74. [PubMed: 8033213]
20. Loda M, Cukor B, Tam SW, et al. Increased proteasome-dependent degradation of the cyclin-dependent kinase inhibitor p27 in aggressive colorectal carcinomas. Nat Med. 1997; 3:231–234. [PubMed: 9018245]
21. Porter PL, Malone KE, Heagerty PJ, et al. Expression of cell-cycle regulators p27Kip1 and cyclin E, alone and in combination, correlate with survival in young breast cancer patients. Nat Med. 1997; 3:222–225. [PubMed: 9018243]
22. Chu IM, Hengst L, Slingerland JM. The Cdk inhibitor p27 in human cancer: prognostic potential and relevance to anticancer therapy. Nat Rev Cancer. 2008; 8:253–267. [PubMed: 18354415]
23. Philipp-Staheli J, Kim KH, Payne SR, et al. Pathway-specific tumor suppression. Reduction of p27 accelerates gastrointestinal tumorigenesis in Apc mutant mice, but not in Smad3 mutant mice. Cancer Cell. 2002; 1:355–368. [PubMed: 12086850]
24. Yan Y, Zhang X, Legerski RJ. Artemis interacts with the Cul4A-DDB1DDB2 ubiquitin E3 ligase and regulates degradation of the CDK inhibitor p27. Cell Cycle. 2011; 10:4098–4109. [PubMed: 22134138]
25. Higa LA, Mihaylov IS, Banks DP, et al. Radiation-mediated proteolysis of CDT1 by CUL4-ROC1 and CSN complexes constitutes a new checkpoint. Nat Cell Biol. 2003; 5:1008–1015. [PubMed: 14578910]
26. Nishitani H, Sugimoto N, Roukos V, et al. Two E3 ubiquitin ligases, SCF-Skp2 and DDB1-Cul4, target human Cdt1 for proteolysis. EMBO J. 2006; 25:1126–1136. [PubMed: 16482215]
27. Hu J, McCall CM, Ohta T, et al. Targeted ubiquitination of CDT1 by the DDB1-CUL4A-ROC1 ligase in response to DNA damage. Nat Cell Biol. 2004; 6:1003–1009. [PubMed: 15448697]
28. Delaval B, Doxsey SJ. Pericentrin in cellular function and disease. J Cell Biol. 2010; 188:181–190. [PubMed: 19951897]
29. To MD, Quigley DA, Mao JH, et al. Progressive genomic instability in the FVB/Kras(LA2) mouse model of lung cancer. Mol Cancer Res. 2011; 9:1339–1345. [PubMed: 21807965]
30. Garnis C, Lockwood WW, Vucic E, et al. High resolution analysis of non-small cell lung cancer cell lines by whole genome tiling path array CGH. Int J Cancer. 2006; 118:1556–1564. [PubMed: 16187286]
31. Cang Y, Zhang J, Nicholas SA, et al. DDB1 is essential for genomic stability in developing epidermis. Proc Natl Acad Sci U S A. 2007; 104:2733–2737. [PubMed: 17301228]
32. Cang Y, Zhang J, Nicholas SA, et al. Deletion of DDB1 in mouse brain and lens leads to p53-dependent elimination of proliferating cells. Cell. 2006; 127:929–940. [PubMed: 17129780]
33. Kotake Y, Zeng Y, Xiong Y. DDB1-CUL4 and MLL1 mediate oncogene-induced p16INK4a activation. Cancer Res. 2009; 69:1809–1814. [PubMed: 19208841]
34. Esteller M, Sanchez-Cespedes M, Rosell R, et al. Detection of aberrant promoter hypermethylation of tumor suppressor genes in serum DNA from non-small cell lung cancer patients. Cancer Res. 1999; 59:67–70. [PubMed: 9892187]
35. Andujar P, Wang J, Descatha A, et al. p16INK4A inactivation mechanisms in non-small-cell lung cancer patients occupationally exposed to asbestos. Lung Cancer. 2010; 67:23–30. [PubMed: 19375815]
36. Martin-Caballero J, Flores JM, Garcia-Palencia P, et al. Tumor susceptibility of p21(Waf1/Cip1)-deficient mice. Cancer Res. 2001; 61:6234–6238. [PubMed: 11507077]
37. Soucy TA, Smith PG, Milhollen MA, et al. An inhibitor of NEDD8-activating enzyme as a new approach to treat cancer. Nature. 2009; 458:732–736. [PubMed: 19360080]
38. Belani CP, Langer C. Group TAXS. First-line chemotherapy for NSCLC: an overview of relevant trials. Lung Cancer. 2002; 38(Suppl 4):13–19. [PubMed: 12480190]
39. Schiller JH, Harrington D, Belani CP, et al. Comparison of four chemotherapy regimens for advanced non-small-cell lung cancer. N Engl J Med. 2002; 346:92–98. [PubMed: 11784875]
40. Nawrocki ST, Kelly KR, Smith PG, et al. Disrupting protein NEDDylation with MLN4924 is a novel strategy to target cisplatin resistance in ovarian cancer. Clin Cancer Res. 2013; 19:3577–3590. [PubMed: 23633453]

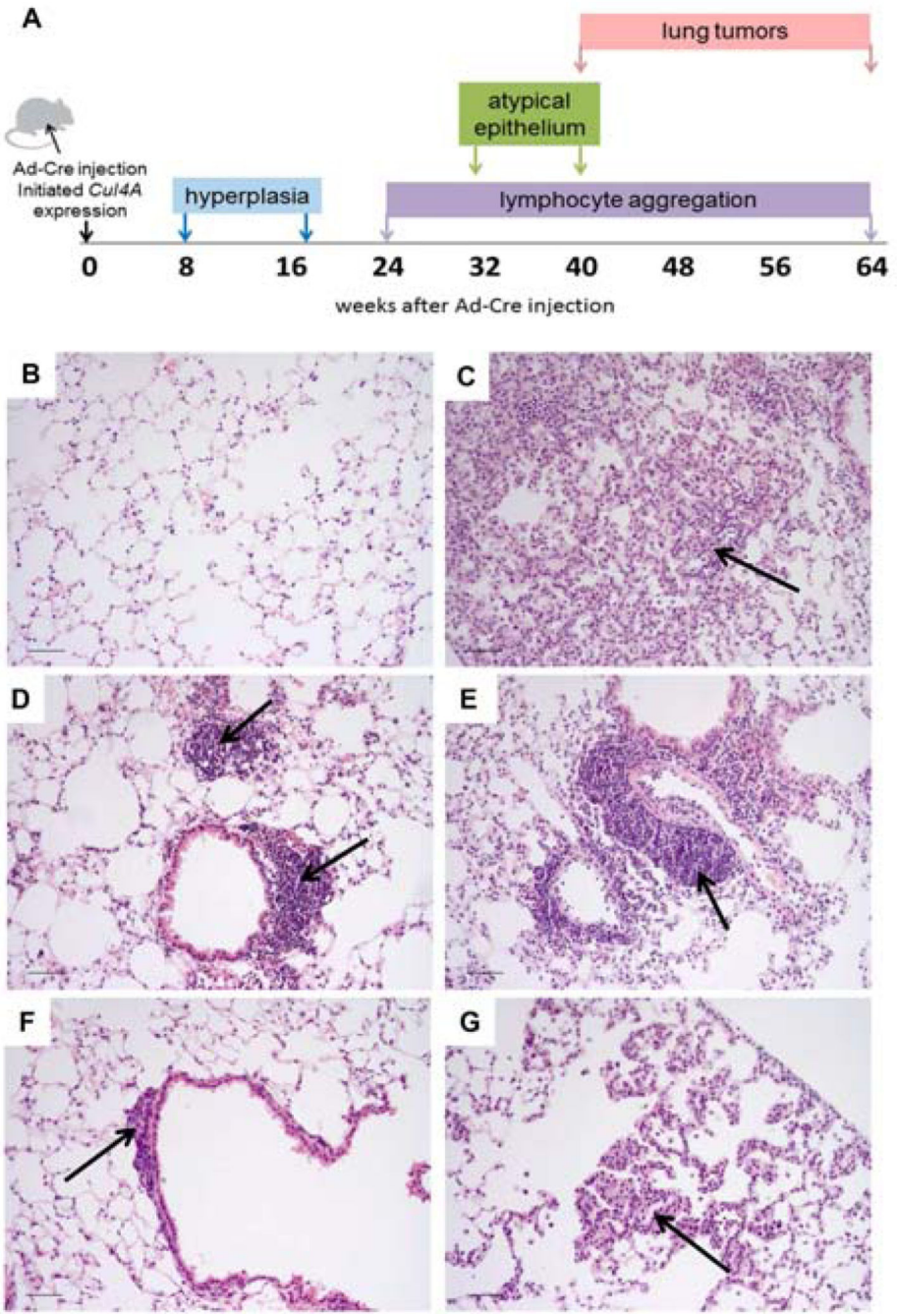

Figure 1.

Morphology of *Cul4A* transgenic mouse lungs. (A) A summary of lung morphology after *Cul4A* overexpression was induced. (B) Alveolar structure is normal in Ad-GFP induced mouse lung at 32 weeks post-induction, whereas (C) the Ad-Cre induced mouse lung at 40 weeks showed alveolar edema (arrow). (D) Lymphocyte aggregations (arrows) near respiratory epithelium were present in Ad-Cre induced mouse lungs at 24 weeks, and (E) the aggregation was enlarged at 40 weeks (arrow). Atypical epithelial cells (arrows) were observed in Ad-Cre induced mouse lungs (F) at 32 weeks (arrow) and (G) 40 weeks (arrow).

Cell nuclear size and cell size were enlarged in the atypical epithelial cells compared to the nearby respiratory epithelium. Images were captured at 20× magnification. (Scale bar: 50μm)

A

	T1	T2	T3	T4	T5	T6	T7	T8	T9
Week	40	48	56	56	64	64	64	64	64
Grade	GRII	GRI	GRI	GRII	GRII	GRII	GRII	GRI	NA
Size (mm)	NA	3x2	2x2	NA	4x4	1.5x1.5	NA	5x5	NA

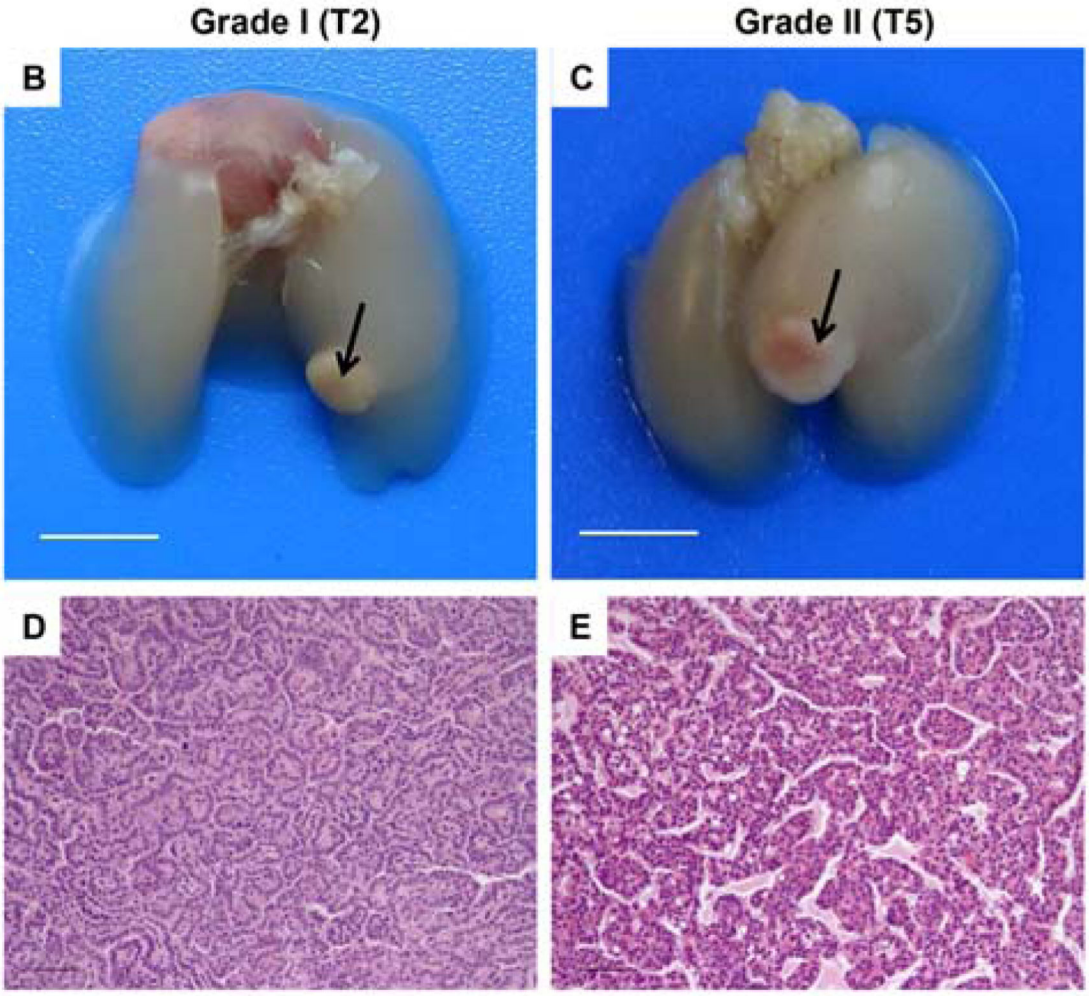

Figure 2.

Lung tumors in the Ad-Cre induced *Cul4A* transgenic mouse. (A) A summary of nine tumors (T1-T9) isolated from the mouse lungs. Samples with unknown tumor grade or tumor size were labeled as NA. (B,C) Tumors were identified in Ad-Cre induced mouse lungs (arrow) while the majority of the lung surface remained smooth. (Scale bar: 5mm) (B) The lung tumor observed at 48 weeks post-induction was characterized as Grade I adenocarcinoma with (D) well-differentiated tumor cells (Grade I, T2). (C) The lung tumor observed at 64 weeks post-induction was characterized as Grade II adenocarcinoma with (E)

moderately differentiated tumor cells (Grade II, T5). Images were captured at 20× magnification. (Scale bar: 50μm)

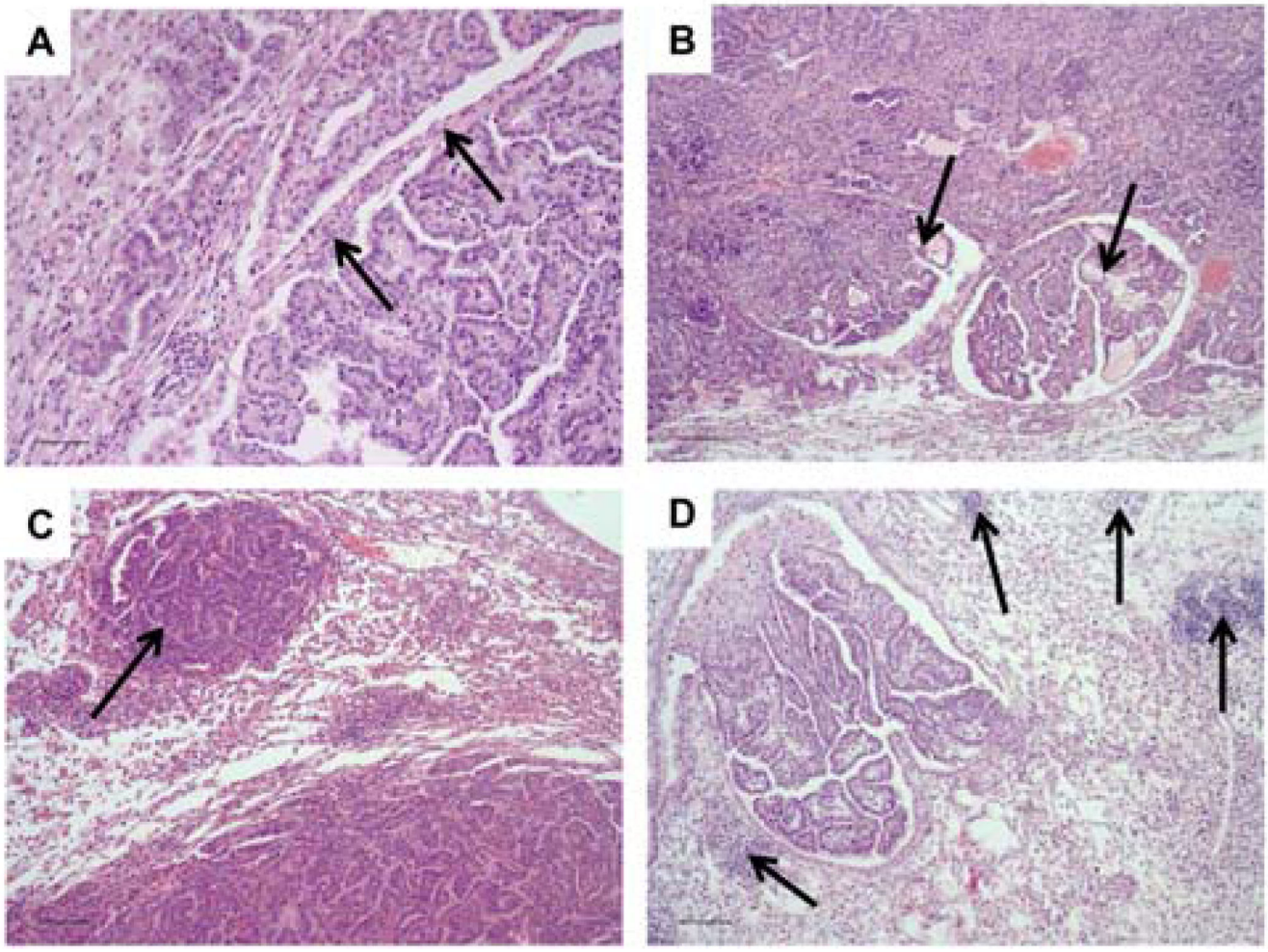

Figure 3.

Tumor-associated changes in the lungs of Ad-Cre induced *Cul4A* transgenic mice. (A) Groups of tumor cells were observed outside of the tumor barrier (arrows) (20× magnification; Scale bar: 50μm). (B) Tumor cells were observed in the lymphatic channels (10× magnification; Scale bar: 100μm). (C) A tumor island (arrow) was observed near the main tumor (10× magnification; Scale bar: 100μm). (D) Lymphocyte aggregations (arrows) were observed surrounding the developed adenocarcinoma (10× magnification; Scale bar: 100μm).

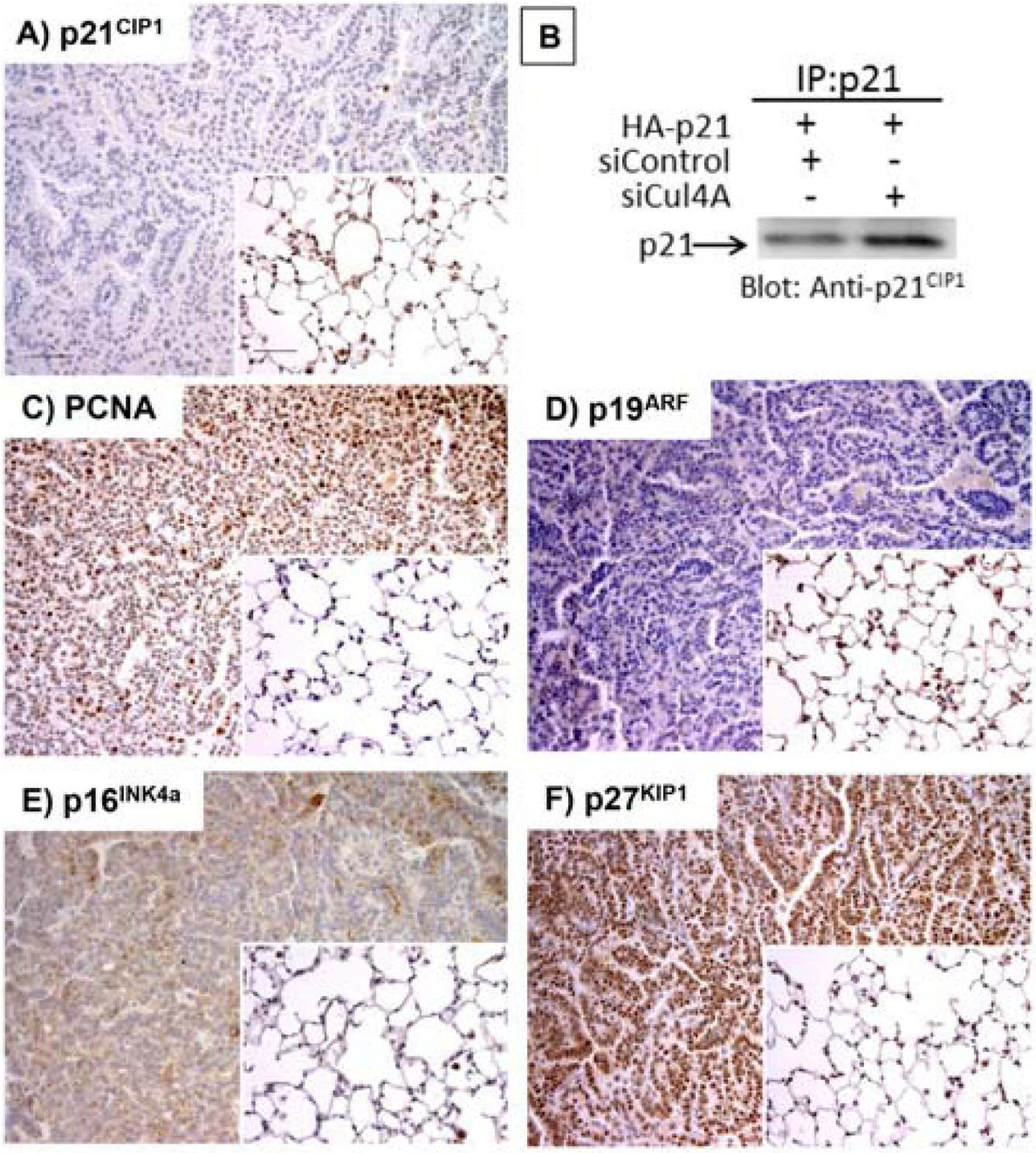

Figure 4.

IHC analysis of Ad-Cre induced *Cul4A* mouse lung tumors and control lungs. Samples were immunostained with antibody specific to (A) $p21^{CIP1}$, (C) PCNA, (D) $p14/p19^{ARF}$, (E) $p16^{INK4a}$, (F) $p27^{KIP1}$. Expression of each protein was analyzed in lung tumors from Ad-Cre induced mouse lungs (main figure) and in the control Ad-GFP induced mouse lungs (inset). Images were captured at 20× magnification. (Scale bar: 50μm) (B) Western blotting of $p21^{CIP1}$ in primary MEFs co-transfected with HA-$p21^{CIP}$1-pcDNA3 plasmid and either *Cul4A* siRNA or control siRNA.

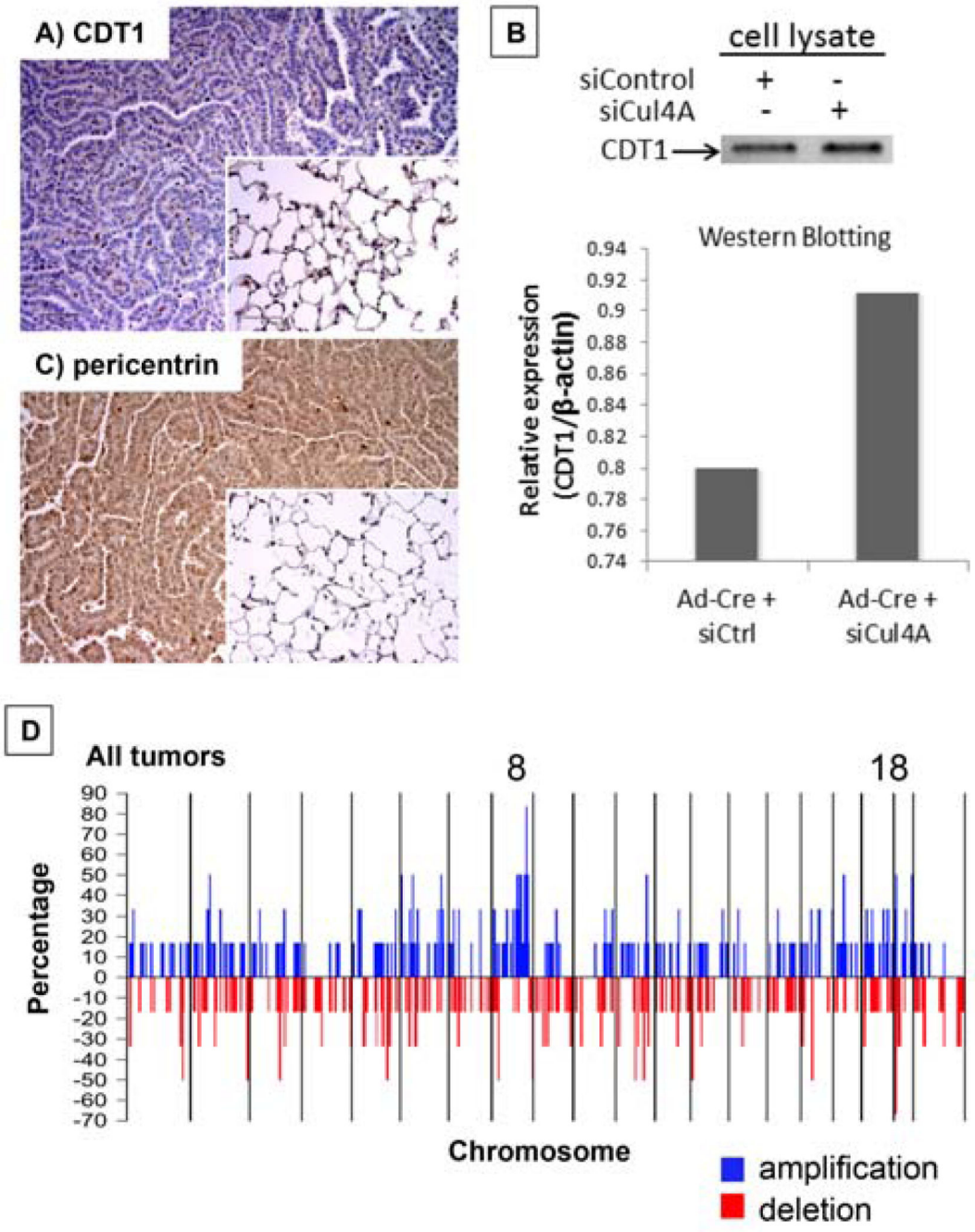

Figure 5.

Genomic instability in lung tumors from the *Cul4A* transgenic mice. Expression of (A) CDT1 and (C) pericentrin was analyzed by IHC in tumor samples from Ad-Cre induced mouse lungs (main figure) and in the control Ad-GFP induced mouse lungs (inset). Images were captured at 20× magnification (Scale bar: 50μm). (B) Western blotting of CDT1 in primary MEFs transfected with either *Cul4A* siRNA or control siRNA. CDT1 expression was quantitated and normalized to β-actin expression. (D) Percentage of tumors with DNA

copy number alterations at each locus across the genome was analyzed with aCGH in six tumors that overexpressed *Cul4A*.

A

	H2170	H345	H226	H838	A549	H460
Copy number	4	3	3	2	2	2
IHC score	+++	++	+++	++	++	++

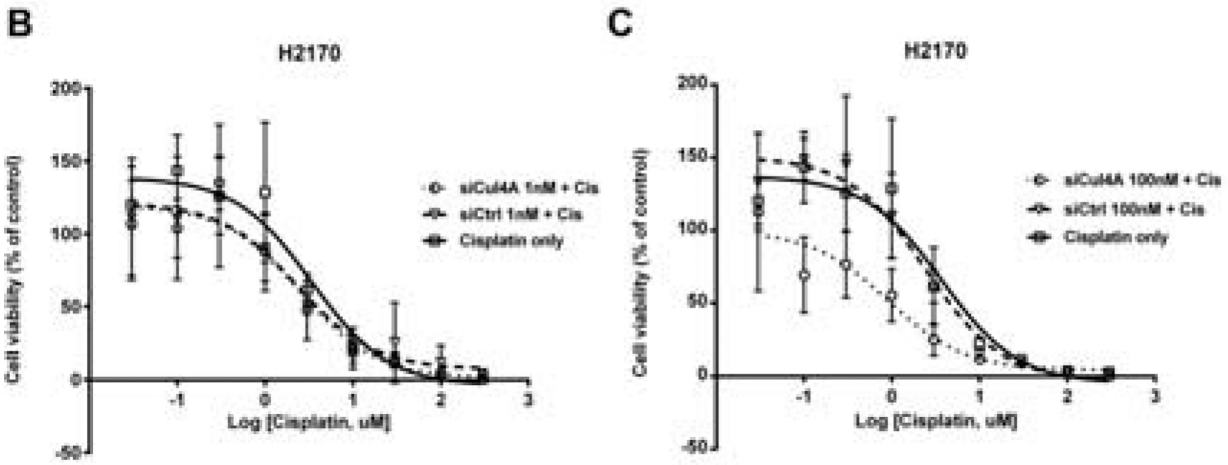

D

	siCul4A 100nM + Cisplatin	siCtrl 100nM + Cisplatin	siCul4A 1nM + Cisplatin	siCtrl 1nM + Cisplatin	Cisplatin only
IC_{50} [μm]	0.91 ± 5.8	2.34 ± 5.5	2.48 ± 5.1	2.31 ± 56.5	3.35 ± 5.3
p value	0.02	>0.05	>0.05	>0.05	

Figure 6.

Cul4A copy number in lung cancer cell lines and inhibition effects of cisplatin on cellular viability. (A) *Cul4A* expression was scored from moderate (++) to high (+++) in six lung cancer cell lines after IHC analysis. Among these cell lines, H2170 had the highest copy number of *Cul4A* measured using FISH. H2170 cells were challenged with (B) 1nM siRNA or (C) 100 nM siRNA before treatment with increasing concentrations of cisplatin (Cis) (0.03 μM to 300 μM). Cellular viability was measured after 72 hrs, and data points represent the relative cell numbers after the treatment (percentage to control). (D) IC_{50} was calculated

based on the cellular viability curve. H2170 cells treated with 0.1% DMSO were used as a control and the percentage of cells in this group was set as 100%. Data points of *Cul4A* siRNA (solid circle with dotted line), control siRNA (solid triangle with dashed line), and cisplatin only (solid square with solid line) were presented. The assay was done in triplicate and bars indicate SD.

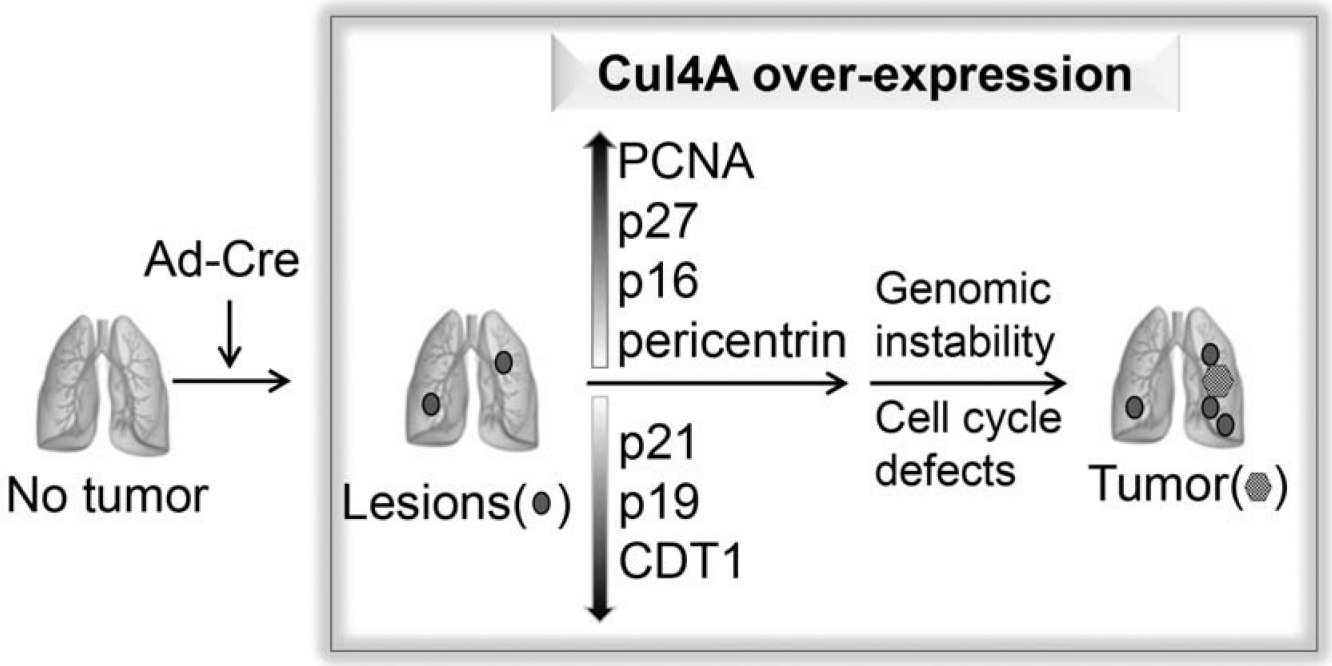

Figure 7.

Schematic explanation of potential mechanisms of initiation and progression of lung tumor in Ad-Cre induced *Cul4A* transgenic mice. Lungs from the transgenic mice appear to be normal without tumor until *Cul4A* overexpression was induced by Ad-Cre. Lesions were observed in the lungs in which *Cul4A* was overexpressed, including alveolar edema, lymphocyte aggregation, and atypical epithelial cells. Decreased levels of $p21^{CIP1}$, $p19^{ARF}$ and CDT1 proteins and increased levels of PCNA, $p27^{KIP1}$, $p16^{INK4a}$, and pericentrin proteins contributed to cell-cycle defects and genomic instability, resulting in tumor development in the lungs in which *Cul4A* was overexpressed.